Acvr1b loss promotes formation of precancerous lesions from acinar and ductal cells of origin

Kiyoshi Saeki[1,2,3], Shilpa Patil[4], Yanping Sun[5], Gloria H. Su[1,2,3], and Janel L. Kopp[4,†]

[1] The Department of Pathology and Cell Biology, Columbia University Irving Medical Center, New York, NY 10032, USA.
[2] Herbert Irving Comprehensive Cancer Center, Columbia University Irving Medical Center, New York, NY 10032, USA.
[3] Department of Otolaryngology and Head and Neck Surgery, Columbia University Irving Medical Center, New York, NY 10032, USA.
[4] Department of Cellular and Physiological Sciences, Life Sciences Institute, University of British Columbia, Vancouver, Canada V6T 1Z3
[5] Oncology Precision Therapeutics and Imaging Core (OPTIC), Columbia University Medical Center, New York, NY 10032, USA

[†]Corresponding author:
Janel Kopp
2350 Health Sciences Mall
Vancouver, BC Canada V6T 1Z3
E-mail: janelk@mail.ubc.ca
Telephone: (604) 827-0626
Fax: 604-822-2316

Funding: The project was supported by NIH grants to G.H.S. and CIHR grants to J.L.K. (MOP-142216 and PJT-162239). J.L.K. was supported by a CIHR New Investigator Award (Msh-147794) and the MSFHR Scholar Award (18309).

Author Contributions: K.S. and G.H.S. designed, managed, and conducted the project including acquiring and interpreting the majority of the data and drafting the manuscript. Y.S. assisted with acquiring and interpreting MRI data. S.P. assisted with figure preparation and editing. J.L.K. and G.H.S. supervised the

project, obtained funding, interpreted the data, and edited the manuscript. K.S. and J.L.K. are the guarantor of this work.

Data transparency: All the authors have access to the study data and have reviewed and approved the final manuscript. Original data and materials will be provided on request.

Disclaimer: This work was prepared while Gloria Su was employed at Columbia University Irving Medical Center. The opinions expressed in this article are the author's own and do not reflect the view of the National Institutes of Health, the Department of Health and Human Services, or the United States government.

Acknowledgements: The authors thank members from Su and Kopp labs for discussions. We thank Christopher Wright (Vanderbilt, USA) for the *Ptf1a*^{CreER} mice and Maike Sander for the *Sox9CreER* mice. We thank the Histology Service Core Facility at CUIMC.

Conflict of interest: The authors report no relevant conflicts of interest.

Body word count: 3764 (without methods)

Abbreviations:

ACVR1B - Activin receptor-like kinase 4
IHC - Immunohistochemistry
IPMN - Intraductal Papillary Mucinous Neoplasm
MCN - Mucinous Cystic Neoplasm
MIP - Maximum Intensity Projection
MRI – Magnetic resonance imaging
PanIN - Pancreatic Intraepithelial Neoplasia
PDAC - Pancreatic ductal adenocarcinoma
TE - Echo time
TGF-β - Transforming growth factor - beta
TR - Repetition time

Abstract

Objective: Pancreatic ductal adenocarcinoma (PDAC) can develop from precursor lesions, such as pancreatic intraepithelial neoplasia (PanIN), mucinous cystic neoplasm (MCN), and intraductal papillary mucinous neoplasm (IPMN), with IPMN having a more favorable prognosis. Previous studies indicated that loss of *Acvr1b* accelerates the development of Kras-induced IPMN in the mouse pancreas, however, the cell type predominantly affected by these genetic changes remains unclear.

Design: We investigated the contribution of cellular origin by inducing IPMN associated mutations- $KRAS^{G12D}$ expression and *Acvr1b* loss specifically in acinar (*Ptf1a*^{CreER};*Kras*$^{LSL\text{-}G12D}$;*Acvr1b*$^{fl/fl}$ mice) or ductal (*Sox9CreER;Kras*$^{LSL\text{-}G12D}$;*Acvr1b*$^{fl/fl}$ mice) cells in mice. We then performed MRI imaging and a thorough histopathological analysis of their pancreatic tissues.

Results: The loss of *Acvr1b* increased the risk of developing PanIN from cells with a Kras mutation. This was more pronounced in the context of acinar cells, which progressed faster and formed cysts that developed into IPMN and tumors. Ductal cells developed fewer PanIN lesions, and progressed less frequently into cysts, but were associated with dilation of the main pancreatic duct. Immunohistochemistry revealed that lesions arising from both cell types exhibited features of gastric or pancreatobiliary epithelium. The caerulein treatment further accelerated the development of IPMN from acinar cells with mutant Kras and loss of *Acvr1b,* but had no effect in ductal cells.

Conclusion: These findings indicate that loss of *Acvr1b* in the presence of the Kras oncogene promotes the development of precancerous lesions from both ductal and acinar cells, with lesions being more prevalent from acinar cells. Our study underscores the significance of the cellular context in the initiation and progression of precursor lesions from adult exocrine cells.

Keywords: intraductal papillary mucinous neoplasm (IPMN), pancreas, carcinogenesis, cellular origin

Introduction

Pancreatic cancer initiation is associated with three main types of precancerous lesions – Pancreatic Intraepithelial Neoplasia (PanIN), Intraductal Papillary Mucinous Neoplasm (IPMN) and Mucinous Cystic Neoplasm (MCN). Adult pancreatic ductal and acinar cells can both give rise to precancerous lesions in animal models (1-5) when mutations in *Kras*, the most commonly altered oncogene in pancreatic cancer, are present. However, the majority of gene mutations and pathway alterations associated with pancreatic cancer have been studied in the context of pan-pancreatic genetic changes induced during pancreatogenesis (6). Thus, how a particular gene affects the initiation and development of precancerous lesions and pancreatic cancer from either acinar or especially ductal cells is largely unknown.

Activin receptor-like kinase 4 (ACVR1B), is a member of the transforming growth factor - beta (TGF-β) superfamily of receptor serine/threonine kinase. Compared to the TGF-β and BMP pathways within the TGF-β superfamily, our understanding of activin signaling is not as comprehensive. Activins exert their effect by binding to either ACVR2A or ACVR2B (Type II receptors), which prompts the recruitment of a type I receptor like ACVR1B. The activated receptor complex then activates SMAD2 and SMAD3, which forms a complex with SMAD4 and regulates gene transcription in the nucleus. Activin signaling plays a crucial role in several cellular processes such as cell proliferation (7-9), cell cycle arrest (10), and apoptosis (11, 12). Dysregulation of activin signaling components has been implicated in several diseases, including cancer. Biallelic inactivation of ACVR1B has been reported in pancreatic cancer (13, 14). Mutations in SMAD2/3/4, which are downstream mediators of activin/TGFβ signaling, are also found in many cancers (15), with 55% of pancreatic cancers having SMAD4 loss (16). Loss of SMAD4 was primarily found in PDAC, but not the precancerous lesions. However, both *Smad4* loss and *Acvr1b* loss in the pancreas using animal models is associated with the development of PanIN lesions, cystic pancreatic precursors, and pancreatic cancer development in the context of oncogenic Kras, suggesting that the Activin arm of TGFβ superfamily can affect the initiation and development of precursor lesions.

In our previous studies, we showed that loss of *Acvr1b* in mouse pancreas, when combined with oncogenic Kras, promoted IPMN formation and pancreatic cancer (17). These data suggested that *Acvr1b* is important in suppressing the early stages of pancreatic tumorigenesis. Our previous studies used the *Pdx1-cre* mouse line, which is expressed in early pancreatic progenitor cells, resulting in the genetic changes occurring in the developing endocrine, acinar, and ductal cells. This made it unclear which specific cell type gave rise to the IPMN in the absence of *Acvr1b*. To address the consequence of *Acvr1b* loss specifically in acinar or ductal cells in the pancreas in the context of oncogenic Kras, we crossed $Kras^{LSL\text{-}G12D}$;$Acvr1b^{fl/fl}$ mice to mice expressing the CreER protein in an acinar- or ductal-cell-specific manner and examined the development of lesions. We found that *Acvr1b* loss and activation of *Kras* in either the acinar or ductal cells promotes precancerous lesion formation. In addition, we found that branch-type IPMN subtype could originate from the acinar cells, while the main duct IPMN was associated with a ductal cell origin, in the absence of *Acvr1b*. In sum, our data suggests Activin signaling is important for limiting initiation of pancreatic precursor lesions from both exocrine cell types.

Results

Acvr1b loss and activation of Kras in acinar cells promotes formation of PanIN and IPMN-like precancerous lesions

To determine whether *Acvr1b* loss promotes lesion formation from $Kras^{G12D}$-expressing acinar cells, we generated a mouse model in which a shared set of IPMN-associated genetic changes in *Kras* and *Acvr1b* were induced in an acinar-cell-type-specific manner. Specifically, we used the tamoxifen-inducible $Ptf1a^{CreER}$ allele to induce Cre-dependent recombination of the $Kras^{LSL\text{-}G12D}$ and $Acvr1b^{flox}$ conditional alleles to express $Kras^{G12D}$ and ablate *Acvr1b* expression (Fig. 1A) in acinar cells. By combining all of these alleles through cross-breeding and injecting the offspring with tamoxifen at 3 to 4 weeks of age, we generated $Ptf1a^{CreER}$;$Kras^{LSL\text{-}G12D}$;$Acvr1b^{fl/fl}$ mice (AKpt) (Fig. 1A). Mice injected with tamoxifen, but lacking the $Acvr1b^{flox}$ alleles, were used as controls ($Ptf1a^{CreER}$;$Kras^{LSL\text{-}G12D}$) (Kpt).

The survival studies in AKpt mice (n=20) indicated that these animals had a median survival of 363 days. (Table S1). This is shorter than the reported median survival of *Pdx1Cre;Kras*^{G12D} mice (~400 days) (22), suggesting that *Acrv1b* loss in acinar cells does reduce survival time in AKpt mice. Upon necropsy, we found multiple cysts present throughout the AKpt pancreas (Fig. 1B). Pancreata were then histologically characterized at various ages (Fig. 1C). At 3 months of age some AKpt mice had developed ADM and low-grade PanIN lesions. In 5-month-old AKpt mice slightly dilated low-grade PanIN lesions were present and some had with papillary structures within the ductal lumen. In 9-month-old AKpt mice, there were multiple cystic lesions with papillary structures. These epithelia had various types of dysplasia, and at 12 months of age small and large mucinous lesions were widespread (Fig. 1C) and invasive carcinoma was observed (data not shown). In contrast, we noted only the presence of ADM and low-grade PanIN lesions in 7-month-old Kpt mice (Fig. 1D). Even at 9 and 12 months of age, Kpt mice only had ADM and low-grade PanIN lesions (Fig. 1D). These results indicate that the combined effect of Kras mutation and *Acvr1b* loss in acinar cells promoted formation of precancerous lesions.

We quantified the histological changes in the ductal lumens in AKpt mice at different ages (3, 5, 7, and 9 months) by measuring their diameter and subcategorizing the structures into four size groups: 0-500 µm, 500-1000 µm, 1000-2000 µm and >2000 µm (Fig. 1E) (Table S2). At 3 months of age, all the preneoplastic structures were smaller than 500 µm (Fig. 1E). However, from 5 months of age onwards, we observed preneoplastic structures larger than 500 µm, with an increase in the overall number of structures as the AKpt mice got older. Additionally, we observed some abnormal ductal structures larger than 2000 µm at the age of 9 months. Altogether, these findings suggested that the preneoplastic lesions in AKpt mice can progress from an ADM and low-grade PanIN state into an IPMN-like state at later time points. We further compared the number and size of preneoplastic structures in AKpt (n=3) and Kpt mice (n=3) at the age of 9 months (Fig. 1F and Table S3). We found that AKpt mice had more preneoplastic structures larger than 500 µm when compared to Kpt mice, as well as more significantly preneoplastic lesions overall (Fig. 1F). These data suggest

that loss of *Acvr1b* in Kras^{G12D}-expressing acinar cells promotes preneoplastic formation overall and is predisposed to form IPMN-like lesions at later ages. Based on the differences in lumen size between AKpt and Kpt mice, we suggest that neoplastic structures less than 500 μm in size be classified as PanIN, while those larger than 500 μm be classified as IPMN-like in these mouse models.

Acvr1b loss and activation of Kras also promotes induction of precancerous lesions from ductal cells

Next, we examined whether loss of *Acvr1b* promoted PanIN and IPMN-like lesion formation from Kras^{G12D}-expressing ductal cells. Cre-mediated recombination was induced in adult duct cells using the tamoxifen-inducible *Sox9CreER* allele. (19) By combining this allele with the conditional alleles for activating Kras and ablating *Acvr1b*, we generated *Sox9CreER;Kras$^{LSL\text{-}G12D}$;Acvr1b$^{fl/fl}$* (AKsox9) mice (Fig. 2A). *Sox9CreER;Kras$^{LSL\text{-}G12D}$* mice (Ksox9) lacking the *Acvr1b* alleles were used as controls. All mice were injected with tamoxifen at 3-4 weeks of age. We then monitored the AKsox9 and Ksox9 mice for more than 12 months and none reached their humane endpoints due to growth of a pancreatic tumor and the pancreas at necropsy was relatively normal (Fig. 2B). Of all the mice examined, only one 17-month-old AKsox9 had a large macroscopic cyst (Fig. 2D). We then histologically characterized the pancreata of AKsox9 and Ksox9 mice at 5, 7, 12 months of age (Fig. 2C-D and Fig. S1) and measured the diameter of the preneoplastic lesions in AKsox9 mice at 5, 7, 12, and 17 months of age (Fig. 2E). Consistent with previous studies (5), few PanIN lesions were observed in Ksox9 mice at any age (Fig. S1). At 5 months of age, only one AKsox9 mice had a PanIN lesion and a somewhat enlarged common duct compared to control mice (Fig. 2C and Table S4). At 7, 12, and 17 months of age in AKsox9 mice the number of mice with preneoplastic lesions increased and the number of lesions per mouse also increased (Fig. 2C-E). This suggests that loss of *Acvr1b* promotes Kras^{G12D}-expressing ductal cells to form preneoplastic lesions. We also observed cystic preneoplastic lesions with papillary structures in one or two AKsox9 mice at the ages of 7, 12, and 17 months of age, with some lesions exceeding 500 μm in size (Fig. 2C-E and Table S4). We also observed that the main pancreatic duct was dilated in two AKsox9 mice at 12 or 17 months of age with papillary preneoplastic

lesions (Fig. 2D). Altogether these results suggested that loss of *Acvr1b* in the context of Kras mutations promoted preneoplastic lesion formation from ductal cells. While only a small number of these lesions appear to develop into IPMN-like cysts, these lesions were associated with main pancreatic duct dilation suggesting that the lesions may affect fluid flow through the main duct.

Cystic lesions arising from ductal cells affect the main pancreatic duct

We previously observed that preneoplastic lesions observed in AKpdx1 mice appeared to affect the main pancreatic duct (17), but we not detect any instances of main pancreatic duct dilation or neoplastic lesions within the main pancreatic duct in AKpt mice (Fig. 1C and Fig. S2C). This suggested that the main duct dilation may be specific to ductal cells affected in AKpdx1 mice. To evaluate this, we performed MRI imaging of the pancreas in three different mouse models: AKpdx1 (n=4), AKpt (n=3), and AKsox9 (n=11). In AKpdx1 mice, all four mice imaged had multiple cysts (arrowheads), as well as main pancreatic duct dilation (arrows) (Fig. 3A-B and Table S5). Consistent with our previous studies (17), histological analyses of these AKpdx1 mice confirmed the presence of papillary lesions affecting the main pancreatic duct (Fig. S2A-B). In AKpt mice, two out of three mice had multiple cysts, but no main pancreatic duct dilation was observed in those two cases (Fig. 3B and Table S5). Histological analyses of these mice confirmed the presence of large cysts with a mucinous flat epithelium (Fig. S2C). For the AKsox9 mice imaged, we observed cystic lesions in 4 out of 7 cases and one of the 17-month-old mice had a large cyst and there was clear dilation of the main pancreatic duct (Fig. 3C) (note: these observations were confirmed by histology and included in previous histological quantifications (Fig. 2D-E)). Together these results indicated that *Acvr1b* loss and activation of Kras in ductal cells can initiate cysts that affect the main pancreatic duct.

Preneoplastic lesions induced by *Acvr1b* loss and Kras activation have a gastric or pancreatobiliary phenotype

Low-grade PanIN lesions and MCN lesions have a predominantly gastric type epithelium, while IPMN can be divided into four main epithelial phenotypes: gastric, intestinal, pancreatobiliary, and oncocytic type. Discrimination of these

phenotypes is largely based on size, histological, and morphological features, as well as the immunohistochemical expression pattern of MUC1, MUC2 and MUC5AC (23-32). Because none of the lesions in AKpdx1, AKpt, or AKsox9 mice possessed the highly cellular stroma associated with MCN lesions (33), we focused here on only the histological and immunohistochemical pattern of mucin expression. Histopathological examination of preneoplastic lesions in AKpdx1 (3-month-old), AKpt (12-month-old), and AKsox9 (12-month-old) mice demonstrated that the neoplasia consisted of dilated ducts with a prominent proliferation of epithelial cells comprised of complex papillary projections. The papillary epithelia showed various grades of dysplasia from low grade to high grade (Fig. 1, 2, 4 and Fig. S2). The neoplastic cells in these three mouse models were composed of papillary epithelium with abundant mucinous cytoplasm and were positive for Alcian blue staining (Fig. 4). Immunohistochemical staining for MUC1, MUC2, and MUC5AC (Fig. 4) showed that these lesions expressed MUC1 and MUC5AC, but there was no expression of MUC2 (Fig. 4). In sum, these findings indicate that these preneoplastic lesions have the features of a gastric or pancreatobiliary type epithelium.

Caerulein treatment accelerated formation of IPMN-like lesion from acinar cells in AKpt mice

Acute pancreatitis can be induced by treatment with a cholecystokinin receptor agonist, caerulein. Pancreatitis is known to accelerate the development of ADM/PanIN in the presence of oncogenic Kras and it is a risk factor for pancreatic cancer (5, 21, 34-36). To evaluate the impact of pancreatitis on the formation of PanIN and IPMN-like lesions following acinar cell-specific Kras activation with or without *Acvr1b* loss, we injected tamoxifen at 3-4 weeks of age and then induced caerulein-mediated acute pancreatitis in 6-week-old Kpt (n=5) and AKpt mice (n=5) and analyzed pancreatic tissue 21 days later (Fig. 5A-C). Consistent with previous literature (5), we confirmed that acute pancreatitis resulted in PanIN formation from oncogenic Kras-expressing acinar cells in Kpt mice by day 21 (Fig. 5B). In the AKpt mice, acute pancreatitis increased the replacement of acinar cells with ductal-like cells compared to Kpt mice, and more cystic lesions were observed (Fig. 5B). To quantify the number of acinar cells in AKpt and Kpt mice,

we performed IHC to detect amylase in the pancreas of the caerulein-treated Kpt (n=5) and AKpt mice (n=5) and measured the amylase positive pancreatic areas (Fig. 5C). The percentage of amylase-positive area in the AKpt mice was significantly lower than that of the Kpt mice ($p<0.05$) (Fig. 5D and Table S7). We also performed immunohistochemical staining for CK19 on Kpt (n=5) and AKpt pancreata (n=5) at day 21 and quantified the CK19-positive areas. We found that the proportion of CK19-positive area in the AKpt mice, mostly composed of ADM, PanIN, and IPMN-like cysts, was significantly higher than that of the Kpt mice ($p<0.05$) (Fig. 5E and Table S7). These results indicated that the caerulein treatment accelerated the process of IPMN development from the acinar cells harboring mutant *Kras* and loss of *Acvr1b*.

Precancerous lesions are not induced by caerulein treatment of AKsox9 mice

We previously demonstrated that caerulein-mediated pancreatitis does not promote $Kras^{G12D}$-expressing ductal cells to form PanIN (5). Given that preneoplastic lesion formation is promoted by the absence of *Acvr1b*, we next examined how caerulein-mediated pancreatitis affects PanIN and IPMN formation from $Kras^{G12D}$-expressing ductal cells with or without *Acvr1b* loss. To do this, we injected tamoxifen at 3-4 weeks of age and then induced caerulein-mediated acute pancreatitis in 6-week-old Ksox9 (n= 4-6) and AKsox9 mice (n= 3-4) and analyzed pancreatic tissue 21 days later (Fig. 6A). Similar to what was previously published (5), and in contrast to Kpt mice, similar amounts of inflammation and degranulation of the acinar cells was observed at 2 days after caerulein treatment in both genotypes and we did not detect any PanINs in either Ksox9 or AKsox9 mice 21 days or 9 weeks after caerulein treatment (Fig. 6B). These results suggested that $Kras^{G12D}$-expressing ductal cells have a low propensity to form PanINs even when exposed to conditions pro-neoplastic for $Kras^{G12D}$-expressing acinar cells, such as acute pancreatitis. Additionally, *Acvr1b* loss did not further promote lesion formation from ductal cells in the context of acute pancreatitis.

Discussion

Acvr1b loss and activation of Kras in either the acinar or ductal cell lineages promotes formation of precancerous lesions

Our study demonstrates that loss of *Acvr1b* in adult ductal or acinar cells expressing $Kras^{G12D}$ results in the formation of more precancerous lesions compared to $Kras^{G12D}$ expression alone. In addition, some of the lesions in AKpt and AKsox9 mice become large cystic lesions with flat or papillary mucinous epithelium, consistent with gastric type IPMN. To date, the majority of animal models of pancreatic cancer have focused on examining the effect of cancer associated mutations in all pancreatic cells or by specifically examining the effect in acinar cells (6). Thus, knowledge of how genetic changes affect tumorigenesis are largely based on the effects on all pancreatic cells in the context of an embryonic induction or on adult acinar cells. Relatively recent studies have begun to identify how pancreatic cancer associated genetic changes affect ductal cells contribution to pancreatic cancer *in situ*. The effects of the mutations studied thus far have shown that some of the mutations that affect tumorigenesis from ductal cells have little or the opposite effects on adult acinar cells (20, 37, 38). In our studies, we found that *Acvr1b* loss, likely through abrogation of Activin signaling, is one of the few pathways identified to date that promotes precancerous lesion formation from both acinar and ductal cells expressing $Kras^{G12D}$. Loss of *Tp53* function or *Fbw7* in the context of oncogenic Kras also promotes the initiation of pancreatic cancer from both acinar and ductal cells (39, 40). Since Activin and *Fbw7* function are both associated with p53 function (9, 41), it is possible that p53 function is universally required to limit tumorigenesis from the pancreatic exocrine cells. However, given that there are slight differences in the overall requirement for heterozygous or homozygous loss of function, for at least *Tp*53 (39, 42), it appears likely that the exact role of *Tp53* in suppressing tumorigenesis from each cell of origin could differ. Future studies to further delineate these differences are required to understand how *Tp53* loss promotes tumorigenesis in each context.

Acinar and ductal cells can contribute to formation of IPMN-like lesions

Our data suggests that loss of *Acvr1b* in Kras^{G12D}-expressing ductal or acinar cells can lead to formation of large cystic lesions akin to IPMN lesions. Previous studies have predominately reported that only ductal cells can give rise to IPMN-like lesions, while the same mutations in acinar cells typically induces PanIN lesions or has no effect (20, 38, 43, 44). Rare instances of IPMN-like lesions occurring in the context of acinar-cell specific mutations have been observed ((45-47) and unpublished observation). In our studies, it appears that effects of *Acvr1b* loss on cyst formation is not limited to acinar or ductal cells; but due to the increased effects of Kras^{G12D} on the acinar cell population likely leads to a more consistent and robust phenotype in AKpt mice compared to Aksox9 mice. Specifically, in Akpt mice, precancerous lesions form and grow more rapidly resulting in larger cyst lesions, IPMN, and ultimately tumors. *Acvr1b* loss also promotes more precancerous lesions from Kras^{G12D}-expressing ductal cells, but ductal cells still give rise to far fewer PanIN lesions overall, which reduces the potential number of lesions with the capacity to respond to the absence of *Acrv1b* loss and progress into cysts. In sum, our data strongly supports a model in which Activin receptor signaling in precancerous lesions likely suppresses the survival or the proliferation and expansion of smaller lesions into larger cystic IPMN-like lesions in addition to suppressing lesion initiation from each origin.

IPMN histological phenotype is established at the onset of lesion initiation

Preneoplastic lesions in young AKpt and Kpt mice were classified as ADM and low-grade PanIN lesions and indistinguishable between the genotypes. However, with time preneoplastic lesions in AKpt mice grew significantly larger than 500 μm and eventually became large cystic lesions, while the lesions in older Kpt mice were smaller than 500 μm. In humans, although low grade PanIN and gastric type IPMN are distinct intraductal neoplasms by size (25, 48), distinguishing between them is often a difficult task in daily practice. This is due to their shared features, such as mucinous columnar cells with flat or papillary configuration. The primary means of differentiating PanIN from gastric type IPMN in patients is size, with PanIN being smaller than 0.5 cm and IPMN being larger than or equal to 1.0 cm in diameter (48). Lesions ranging from 0.5 cm to 1 cm in size lined with gastric-

like mucinous epithelium can be classified as incipient IPMN (23, 24, 49), which may also be interpreted as either a large low grade PanIN or small gastric type IPMN. In this study, neoplastic lesions in the early stages of AKpt mice had the same morphology, as the ADM and PanIN lesions of Kpt mice, and with age larger cystic lesions resembling human gastric type IPMN were observed. This suggests that the gastric phenotype of the IPMN is established at the initiation of the smaller lesion. Consistent with the IPMN histological phenotype being established early on, incipient IPMN with intestinal or oncocytic features have been observed (23, 24, 49) and mouse models which develop pancreatobiliary or oncocytic IPMN have been shown to have smaller sized lesions with these histological phenotypes (20). Thus, the early-stage PanIN-like neoplastic lesions in AKpt mice could represent an early developmental stage of gastric type IPMN.

Branch duct IPMN could originate from acinar cells, while main-duct IPMN arises from ductal cells

By the histopathological analysis and MRI image evaluation, we found that the cystic lesions in the AKpt mice were likely branch duct type IPMN (BD-type IPMN) with no involvement of the main duct observed. Most human BD-type IPMN tend to be of the gastric IPMN subtype (30, 50), characterized by papilla lined by epithelium highly similar to gastric foveolar epithelium (23). This suggests that branch duct IPMN could arise predominantly from acinar cells. While less common, gastric type IPMN can also be found in the main duct (51). In the AKsox9 mouse model, we observed that main duct dilation and gastric-type IPMN lesions could co-occur. This suggested that main duct-type IPMN with the histological characteristics of gastric type IPMN may arise from the ductal epithelium.

Acute pancreatitis promotes cystic lesions derived from acinar cells

Here we investigated how caerulein-induced acute pancreatitis affects the induction of IPMN. While the development of cystic lesions increased in AKpt compared to Kpt mice 21 days after caerulein treatment, neither PanIN or cystic lesions were induced by caerulein treatment of AKsox9 or Ksox9 mice. The lack of response in the ductal-cell specific models is consistent with previous studies

demonstrating that caerulein treatments inducing acute pancreatitis do not promote PanIN formation (5). Thus, the lack of cystic neoplasia in AKsox9 mice after caerulein treatment may be because PanIN lesions were not induced, which precluded the formation of the cystic lesions. Thus, inflammation that primarily affects the transformation of acinar cells into duct-like cells would likely have its biggest effect on IPMN initiation when tumorigenesis is initiated from acinar cells. However, inflammation driven by partial duct ligation can induce proliferation of endogenous ductal cells and promote their transformation into pancreatic cancer (52). To test whether inflammation also has a role in stimulating IPMN formation from ductal cells, experiments to induce proliferation of endogenous ductal cells via injury in the AKsox9 mouse model are needed.

Methods

Mouse Strains

LSL-Kras^{G12D} (18), *Acvr1b*$^{fl/fl}$ (17), *Ptf1a*^{CreER} (Jax No. 019378), and *Sox9CreER* (5, 19, 20) mice have been described in detail previously. To induce recombination, 3-4-week-old mice were administered three subcutaneous injections of tamoxifen (Sigma Aldrich) in corn oil over 5 days (days 1, 3, and 5) at 5 mg/40 g body weight. *Ptf1a*^{CreER}*;Kras*$^{LSL-G12D}$ (Kpt) mice and *Sox9CreER;Kras*$^{LSL-G12D}$ (Ksox9) mice were used as controls for *Ptf1a*^{CreER}*;Kras*$^{LSL-G12D}$*;Acvr1b*$^{fl/fl}$ (AKpt) mice and *Sox9CreER;Kras*$^{LSL-G12D}$*;Acvr1b*$^{fl/fl}$ (AKsox9) mice. No developmental effects were observed in all of these mice. All mice were housed in the Animal Care Facility at Columbia University Irving Medical Center (CUIMC), and the studies were conducted in compliance with the CUIMC Institutional Animal Care and Use Committee (IACUC) guidelines. Specifically, rapid weight loss in adjunct with body condition score less than 3 (Ullman-Cullere et al, Laboratory Animal Science, 1999), debilitating diarrhea, progressive dermatitis, rough hair coat, hunched posture, lethargy or persistent recumbence, coughing, labored breathing, nasal discharge, neurologic signs, bleeding from any orifice, self-induced trauma, shivering, a tumor burden of >10% body weight, ulceration of the tumor and a mean tumor diameter >20 mm was considered as humane end point. If the

animals lost more than 20% of their body weight, were cachectic, unable to obtain food or water, or their ocular and/or respiratory systems were compromised, they were euthanized.

Histological and Immunolabeling Analyses

Murine tissues were fixed overnight in 10% neutral buffered formalin and embedded in paraffin. Routine H&E staining was performed by the Histology Service Core Facility at CUIMC. K.S. evaluated the histology of all sections and G.H.S. and Dr. Wanglong Qiu (University Irvine Medical Center) provided a secondary analysis of key sections.

For histological analyses, one section per mouse was examined in its entirety and the number of neoplastic structures and the tumor size in each mouse pancreatic area were calculated.

Immunohistochemistry was performed using unstained 5-μm sections derived from the formalin-fixed and paraffin-embedded blocks that were deparaffinized in xylene 3 times and rehydrated in ethanol 4 times. Heat-induced antigen retrieval was performed on all slides in Tris-EDTA buffer (0.5% Tween-20, citrate buffer, pH 6.8) in a steamer for 30 minutes. Slides were incubated with Dako peroxidase block buffer to block endogenous peroxidase activity. Primary antibody staining was performed at 4°C overnight. The secondary antibodies were detected with a 40-minute incubation with biotinylated universal secondary antibodies (Dako, Carpinteria, CA) and streptavidin–horseradish peroxidase. Hematoxylin was then used as a counterstain. Slides were dehydrated in ethanol then xylene and mounted with VectaMount permanent mounting medium (Vector Laboratories Burlingame, CA). The following primary antibodies were used for immunohistochemistry: Amylase (1:100, cat: sc-46657, Santa Cruz), CK19 (1:500, cat: ab52625, Abcam), MUC1 (1:100, #BS-1497R, Bioss Inc.), MUC2 (SC-15334, Santa Cruz) and MUC5AC (#BS-7166R, Bioss Inc.).

For quantification of the IHC (CK19 and Amylase), one section per mouse was examined in its entirety and the percentages of the CK19 or Amylase positive

areas in each mouse were calculated by their proportions to the entire section.

For Alcian blue staining, 5-μm sections were deparaffinized and rehydrated as in immunohistochemistry staining. Then slides were stained with Alcian blue solution (1 g Alcian blue in 100 ml 3% glacial acetic acid, pH 2.5) for 30 minutes at room temperature. Counterstaining with 0.1% nuclear fast red solution (0.1 g nuclear fast red and 5 g ammonium sulfate in 100 ml dH2O) was performed for 5 minutes. Slides were dehydrated and mounted.

Caerulein treatment

Acute pancreatitis was induced at 6 weeks of age in AKpt, Kpt, AKsox9, and Ksox9 mice by 2 sets of 6 hourly i.p. caerulein injection (50 μg/kg diluted in saline; Sigma-Aldrich) separated by 24 hours. In this experiment, the final day of the caerulein/saline injection was considered day 0 (5, 21) and the pancreata were collected as indicated.

MRI experiment

MR images were obtained on a Bruker BioSpec 9.4T Magnetic Resonance Imager (Bruker Corp., Billerica, MA). The mice were anesthetized with 1-2% isofluorane mixed with medical air via a nose cone. The concentration of the isoflurane was adjusted during the procedure to maintain the respiration rate in the range of 40-70 breaths/min using a respiration pillow attached to a monitoring system (SA Instruments, Stony Brook, NY). Body temperature was maintained around 37˚C using a flowing water heating pad. Low-resolution T1 weighted scout images were obtained initially. A rapid acquisition with relaxation enhancement sequence was used to acquire a high-resolution T2 weighted images with the following parameters: repetition time (TR) = 4873 ms, echo time (TE) = 60 ms, field of view = 34 × 34 mm, matrix size =256 x 256, slice thickness = 0.4 mm with 30 slices to cover the entire abdomen. Maximum Intensity Projection (MIP) technique was used for the visualization of the cysts.

Statistical Analysis

P values were calculated using the 2-way ANOVA with GraphPad Prism (version

8.0.2). P values <0.05 were determined to be significant.

All authors have access to the study data and have reviewed and approved the final manuscript.

References

1. Ray KC, Bell KM, Yan J, Gu G, Chung CH, Washington MK, et al. Epithelial tissues have varying degrees of susceptibility to Kras(G12D)-initiated tumorigenesis in a mouse model. PLoS One. 2011;6(2):e16786.
2. Habbe N, Shi G, Meguid RA, Fendrich V, Esni F, Chen H, et al. Spontaneous induction of murine pancreatic intraepithelial neoplasia (mPanIN) by acinar cell targeting of oncogenic Kras in adult mice. Proc Natl Acad Sci U S A. 2008;105(48):18913-8.
3. De La OJ, Emerson LL, Goodman JL, Froebe SC, Illum BE, Curtis AB, et al. Notch and Kras reprogram pancreatic acinar cells to ductal intraepithelial neoplasia. Proc Natl Acad Sci U S A. 2008;105(48):18907-12.
4. Gidekel Friedlander SY, Chu GC, Snyder EL, Girnius N, Dibelius G, Crowley D, et al. Context-dependent transformation of adult pancreatic cells by oncogenic K-Ras. Cancer Cell. 2009;16(5):379-89.
5. Kopp JL, von Figura G, Mayes E, Liu FF, Dubois CL, Morris JPt, et al. Identification of Sox9-dependent acinar-to-ductal reprogramming as the principal mechanism for initiation of pancreatic ductal adenocarcinoma. Cancer Cell. 2012;22(6):737-50.
6. Xu Y, Liu J, Nipper M, Wang P. Ductal vs. acinar? Recent insights into identifying cell lineage of pancreatic ductal adenocarcinoma. Ann Pancreat Cancer. 2019;2.
7. Burdette JE, Jeruss JS, Kurley SJ, Lee EJ, Woodruff TK. Activin A mediates growth inhibition and cell cycle arrest through Smads in human breast cancer cells. Cancer Res. 2005;65(17):7968-75.
8. Yamato K, Koseki T, Ohguchi M, Kizaki M, Ikeda Y, Nishihara T. Activin A induction of cell-cycle arrest involves modulation of cyclin D2 and p21CIP1/WAF1 in plasmacytic cells. Mol Endocrinol. 1997;11(8):1044-52.

9. Zauberman A, Oren M, Zipori D. Involvement of p21(WAF1/Cip1), CDK4 and Rb in activin A mediated signaling leading to hepatoma cell growth inhibition. Oncogene. 1997;15(14):1705-11.
10. Togashi Y, Kogita A, Sakamoto H, Hayashi H, Terashima M, de Velasco MA, et al. Activin signal promotes cancer progression and is involved in cachexia in a subset of pancreatic cancer. Cancer Lett. 2015;356(2 Pt B):819-27.
11. Ying S, Zhang Z, Batres Y, Zhao Y, Lin S, Li G. p53 is involved in the inhibition of cell proliferation mediated by activin A in cultured human prostate cancer LNCaP cells. Int J Oncol. 1997;11(3):591-5.
12. Valderrama-Carvajal H, Cocolakis E, Lacerte A, Lee EH, Krystal G, Ali S, et al. Activin/TGF-beta induce apoptosis through Smad-dependent expression of the lipid phosphatase SHIP. Nat Cell Biol. 2002;4(12):963-9.
13. Su GH, Bansal R, Murphy KM, Montgomery E, Yeo CJ, Hruban RH, et al. ACVR1B (ALK4, activin receptor type 1B) gene mutations in pancreatic carcinoma. Proc Natl Acad Sci U S A. 2001;98(6):3254-7.
14. Togashi Y, Sakamoto H, Hayashi H, Terashima M, de Velasco MA, Fujita Y, et al. Homozygous deletion of the activin A receptor, type IB gene is associated with an aggressive cancer phenotype in pancreatic cancer. Mol Cancer. 2014;13:126.
15. Samanta D, Datta PK. Alterations in the Smad pathway in human cancers. Front Biosci (Landmark Ed). 2012;17(4):1281-93.
16. Blackford A, Serrano OK, Wolfgang CL, Parmigiani G, Jones S, Zhang X, et al. SMAD4 gene mutations are associated with poor prognosis in pancreatic cancer. Clin Cancer Res. 2009;15(14):4674-9.
17. Qiu W, Tang SM, Lee S, Turk AT, Sireci AN, Qiu A, et al. Loss of Activin Receptor Type 1B Accelerates Development of Intraductal Papillary Mucinous Neoplasms in Mice With Activated KRAS. Gastroenterology. 2016;150(1):218-28 e12.
18. Hingorani SR, Petricoin EF, Maitra A, Rajapakse V, King C, Jacobetz MA, et al. Preinvasive and invasive ductal pancreatic cancer and its early detection in the mouse. Cancer Cell. 2003;4(6):437-50.
19. Kopp JL, Dubois CL, Schaffer AE, Hao E, Shih HP, Seymour PA, et al. Sox9+ ductal cells are multipotent progenitors throughout development but do

not produce new endocrine cells in the normal or injured adult pancreas. Development. 2011;138(4):653-65.
20. Kopp JL, Dubois CL, Schaeffer DF, Samani A, Taghizadeh F, Cowan RW, et al. Loss of Pten and Activation of Kras Synergistically Induce Formation of Intraductal Papillary Mucinous Neoplasia From Pancreatic Ductal Cells in Mice. Gastroenterology. 2018;154(5):1509-23 e5.
21. Morris JPt, Cano DA, Sekine S, Wang SC, Hebrok M. Beta-catenin blocks Kras-dependent reprogramming of acini into pancreatic cancer precursor lesions in mice. J Clin Invest. 2010;120(2):508-20.
22. Hingorani SR, Wang L, Multani AS, Combs C, Deramaudt TB, Hruban RH, et al. Trp53R172H and KrasG12D cooperate to promote chromosomal instability and widely metastatic pancreatic ductal adenocarcinoma in mice. Cancer Cell. 2005;7(5):469-83.
23. Adsay V, Mino-Kenudson M, Furukawa T, Basturk O, Zamboni G, Marchegiani G, et al. Pathologic Evaluation and Reporting of Intraductal Papillary Mucinous Neoplasms of the Pancreas and Other Tumoral Intraepithelial Neoplasms of Pancreatobiliary Tract: Recommendations of Verona Consensus Meeting. Ann Surg. 2016;263(1):162-77.
24. Basturk O, Hong SM, Wood LD, Adsay NV, Albores-Saavedra J, Biankin AV, et al. A Revised Classification System and Recommendations From the Baltimore Consensus Meeting for Neoplastic Precursor Lesions in the Pancreas. Am J Surg Pathol. 2015;39(12):1730-41.
25. Adsay NV KG, Fukushima N, et al. Intraductal neoplasms of the pancreas. In: Bosman FT, Carneiro F, Hruban RH, et al, eds. WHO Classification of Tumors of the Digestive System Lyon: WHO Press. 2010:304-13.
26. Noe M, Brosens LAA. Gastric- and intestinal-type IPMN: two of a kind? Virchows Arch. 2020;477(1):17-9.
27. Omori Y, Ono Y, Kobayashi T, Motoi F, Karasaki H, Mizukami Y, et al. How does intestinal-type intraductal papillary mucinous neoplasm emerge? CDX2 plays a critical role in the process of intestinal differentiation and progression. Virchows Arch. 2020;477(1):21-31.
28. Adsay NV, Merati K, Andea A, Sarkar F, Hruban RH, Wilentz RE, et al. The dichotomy in the preinvasive neoplasia to invasive carcinoma sequence in

the pancreas: differential expression of MUC1 and MUC2 supports the existence of two separate pathways of carcinogenesis. Mod Pathol. 2002;15(10):1087-95.
29. Adsay NV, Merati K, Basturk O, Iacobuzio-Donahue C, Levi E, Cheng JD, et al. Pathologically and biologically distinct types of epithelium in intraductal papillary mucinous neoplasms: delineation of an "intestinal" pathway of carcinogenesis in the pancreas. Am J Surg Pathol. 2004;28(7):839-48.
30. Ban S, Naitoh Y, Mino-Kenudson M, Sakurai T, Kuroda M, Koyama I, et al. Intraductal papillary mucinous neoplasm (IPMN) of the pancreas: its histopathologic difference between 2 major types. Am J Surg Pathol. 2006;30(12):1561-9.
31. Ban S, Naitoh Y, Ogawa F, Shimizu Y, Shimizu M, Yasumoto A, et al. Intraductal papillary mucinous neoplasm (IPMN) of the gastric-type with focal nodular growth of the arborizing papillae: a case of high-grade transformation of the gastric-type IPMN. Virchows Arch. 2006;449(1):112-6.
32. Taki K, Ohmuraya M, Tanji E, Komatsu H, Hashimoto D, Semba K, et al. GNAS(R201H) and Kras(G12D) cooperate to promote murine pancreatic tumorigenesis recapitulating human intraductal papillary mucinous neoplasm. Oncogene. 2016;35(18):2407-12.
33. Yonezawa S, Higashi M, Yamada N, Goto M. Precursor lesions of pancreatic cancer. Gut Liver. 2008;2(3):137-54.
34. Guerra C, Schuhmacher AJ, Canamero M, Grippo PJ, Verdaguer L, Perez-Gallego L, et al. Chronic pancreatitis is essential for induction of pancreatic ductal adenocarcinoma by K-Ras oncogenes in adult mice. Cancer Cell. 2007;11(3):291-302.
35. Lowenfels AB, Maisonneuve P, Cavallini G, Ammann RW, Lankisch PG, Andersen JR, et al. Pancreatitis and the risk of pancreatic cancer. International Pancreatitis Study Group. N Engl J Med. 1993;328(20):1433-7.
36. Lowenfels AB, Maisonneuve P, DiMagno EP, Elitsur Y, Gates LK, Jr., Perrault J, et al. Hereditary pancreatitis and the risk of pancreatic cancer. International Hereditary Pancreatitis Study Group. J Natl Cancer Inst. 1997;89(6):442-6.
37. Roy N, Malik S, Villanueva KE, Urano A, Lu X, Von Figura G, et al. Brg1 promotes both tumor-suppressive and oncogenic activities at distinct stages of

pancreatic cancer formation. Genes Dev. 2015;29(6):658-71.
38. von Figura G, Fukuda A, Roy N, Liku ME, Morris Iv JP, Kim GE, et al. The chromatin regulator Brg1 suppresses formation of intraductal papillary mucinous neoplasm and pancreatic ductal adenocarcinoma. Nat Cell Biol. 2014;16(3):255-67.
39. Lee AYL, Dubois CL, Sarai K, Zarei S, Schaeffer DF, Sander M, et al. Cell of origin affects tumour development and phenotype in pancreatic ductal adenocarcinoma. Gut. 2019;68(3):487-98.
40. Ferreira RMM, Sancho R, Messal HA, Nye E, Spencer-Dene B, Stone RK, et al. Duct- and Acinar-Derived Pancreatic Ductal Adenocarcinomas Show Distinct Tumor Progression and Marker Expression. Cell Rep. 2017;21(4):966-78.
41. Mao JH, Perez-Losada J, Wu D, Delrosario R, Tsunematsu R, Nakayama KI, et al. Fbxw7/Cdc4 is a p53-dependent, haploinsufficient tumour suppressor gene. Nature. 2004;432(7018):775-9.
42. Bailey JM, Hendley AM, Lafaro KJ, Pruski MA, Jones NC, Alsina J, et al. p53 mutations cooperate with oncogenic Kras to promote adenocarcinoma from pancreatic ductal cells. Oncogene. 2016;35(32):4282-8.
43. Kimura Y, Fukuda A, Ogawa S, Maruno T, Takada Y, Tsuda M, et al. ARID1A Maintains Differentiation of Pancreatic Ductal Cells and Inhibits Development of Pancreatic Ductal Adenocarcinoma in Mice. Gastroenterology. 2018;155(1):194-209 e2.
44. Collet L, Ghurburrun E, Meyers N, Assi M, Pirlot B, Leclercq IA, et al. Kras and Lkb1 mutations synergistically induce intraductal papillary mucinous neoplasm derived from pancreatic duct cells. Gut. 2020;69(4):704-14.
45. Siveke JT, Einwachter H, Sipos B, Lubeseder-Martellato C, Kloppel G, Schmid RM. Concomitant pancreatic activation of Kras(G12D) and Tgfa results in cystic papillary neoplasms reminiscent of human IPMN. Cancer Cell. 2007;12(3):266-79.
46. Flowers BM, Xu H, Mulligan AS, Hanson KJ, Seoane JA, Vogel H, et al. Cell of Origin Influences Pancreatic Cancer Subtype. Cancer Discov. 2021;11(3):660-77.
47. Ideno N, Yamaguchi H, Ghosh B, Gupta S, Okumura T, Steffen DJ, et

al. GNAS(R201C) Induces Pancreatic Cystic Neoplasms in Mice That Express Activated KRAS by Inhibiting YAP1 Signaling. Gastroenterology. 2018;155(5):1593-607 e12.
48. Hruban RH, Takaori K, Klimstra DS, Adsay NV, Albores-Saavedra J, Biankin AV, et al. An illustrated consensus on the classification of pancreatic intraepithelial neoplasia and intraductal papillary mucinous neoplasms. Am J Surg Pathol. 2004;28(8):977-87.
49. Matthaei H, Wu J, Dal Molin M, Shi C, Perner S, Kristiansen G, et al. GNAS sequencing identifies IPMN-specific mutations in a subgroup of diminutive pancreatic cysts referred to as "incipient IPMNs". Am J Surg Pathol. 2014;38(3):360-3.
50. Furukawa T, Kloppel G, Volkan Adsay N, Albores-Saavedra J, Fukushima N, Horii A, et al. Classification of types of intraductal papillary-mucinous neoplasm of the pancreas: a consensus study. Virchows Arch. 2005;447(5):794-9.
51. Marchegiani G, Mino-Kenudson M, Sahora K, Morales-Oyarvide V, Thayer S, Ferrone C, et al. IPMN involving the main pancreatic duct: biology, epidemiology, and long-term outcomes following resection. Ann Surg. 2015;261(5):976-83.
52. Shi C, Pan FC, Kim JN, Washington MK, Padmanabhan C, Meyer CT, et al. Differential Cell Susceptibilities to Kras(G12D) in the Setting of Obstructive Chronic Pancreatitis. Cell Mol Gastroenterol Hepatol. 2019;8(4):579-94.

Figures

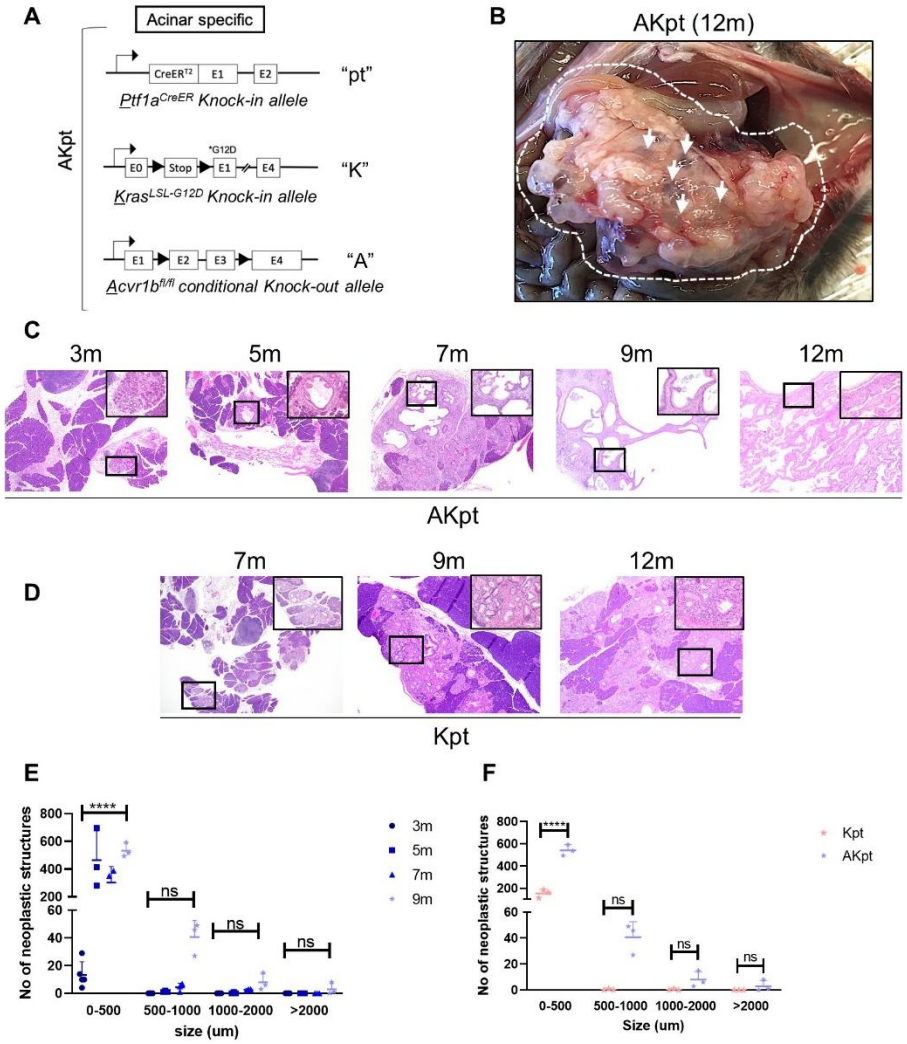

Figure 1. *Acvr1b* loss and activation of Kras in acinar cells promotes initiation of pancreatic cyst with preneoplastic characteristics.

(A) Schematic of the alleles in the *Ptf1a^{CreER};Kras$^{LSL-G12D}$;Acvr1b$^{fl/fl}$* (AKpt) mouse models used in this study. **(B)** Representative gross anatomical photographs of the abdomen from AKpt mouse at 12 months. White dashed line outlines the pancreas with scattered pancreatic cysts (arrows). H&E-stained sections of the AKpt pancreas at 3, 5, 7, 9, and 12 months of age **(C)** or *Ptf1a^{CreER};Kras$^{LSL-G12D}$* (Kpt) mice at 7, 9, and 12 months of age **(D)**. Magnification for main images is 20x and insets are 100x. **(E-F)** Graph depicting the number of the neoplastic structures at different size groups: 0-500 µm, 500-1000 µm, 1000-2000 µm and >2000 µm in AKpt mice at 3 (n=5), 5 (n=3), 7 (n=3), and 9 months of age (n=3) **(E)** or in Kpt (n=3) vs. AKpt mice at the age of 9 months **(F)**. ****=p-value < 0.0001.

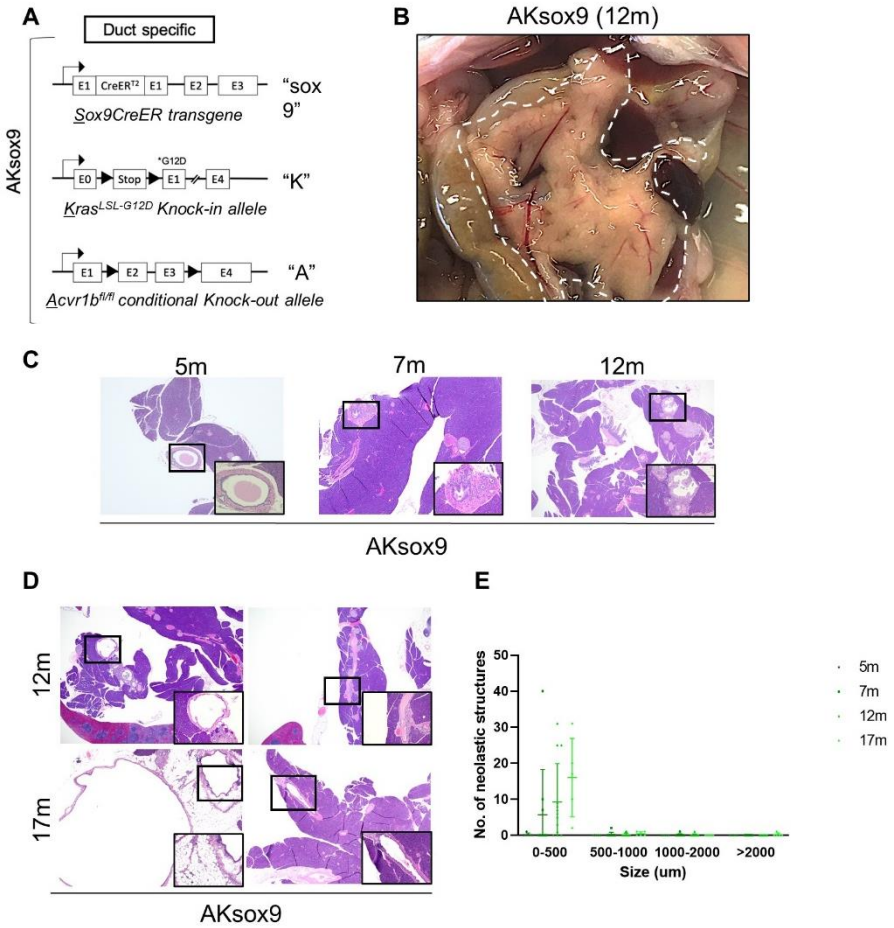

Figure 2. *Acvr1b* loss and activation of Kras in ductal cells promotes formation of preneoplastic lesions and cysts.

(A) Schematic of the alleles in the *Sox9CreER;Kras$^{LSL-G12D}$;Acvr1b$^{fl/fl}$* (AKsox9) mouse models used in this study. **(B)** Representative gross anatomical photographs of the mouse abdomen from AKsox9 mouse at 12 months of age. A dashed white line outlines the pancreatic tissue. **(C)** H&E-stained sections of the AKsox9 pancreata at 5, 7, and 12 months of age. **(D)** H&E-stained sections from AKsox9 mice at 12 or 17 months of age depicting a large cyst (left) and dilation of main pancreatic duct (right). Magnification for main images is 20x and for the insets is 100x. **(E)** Graph depicting the number of neoplastic structures in different size groups: 0-500 µm, 500-1000 µm, 1000-2000 µm, and >2000 µm in the AKsox9 mice at 5 (n=5), 9 (n=10), 12 (n=13), and 17 months of age (n=5).

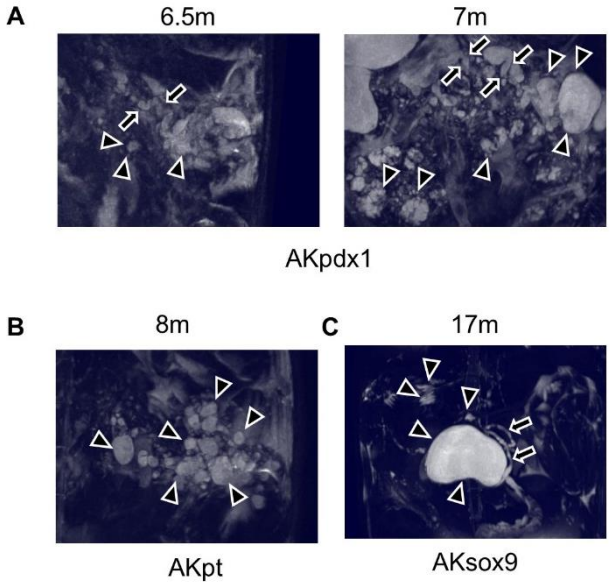

Figure 3. *Acvr1b* loss and activation of Kras in ductal cells is associated with dilation of the main pancreatic duct.

Representative MRI images of the **(A)** *Pdx1Cre;Kras*$^{LSL\text{-}G12D}$*;Acvr1b*$^{fl/fl}$ (AKpdx1) mice at the age of 6.5 and 7 months depicting multiple cystic lesions, as well as dilation of the main pancreatic duct. **(B)** Representative MRI images of the *Ptf1a*^{CreER}*;Kras*$^{LSL\text{-}G12D}$*;Acvr1b*$^{fl/fl}$ (AKpt) mice at the age of 8 months depicting multiple cystic lesions, no main pancreatic duct dilation was observed. **(C)** Representative MRI images of *Sox9CreER;Kras*$^{LSL\text{-}G12D}$*;Acvr1b*$^{fl/fl}$ (AKsox9) mice at 17 months of age depicting multiple cystic lesions, including a big cyst, as well dilation of the main pancreatic duct. The arrowheads indicate cysts. The arrows indicate dilation of the main pancreatic duct.

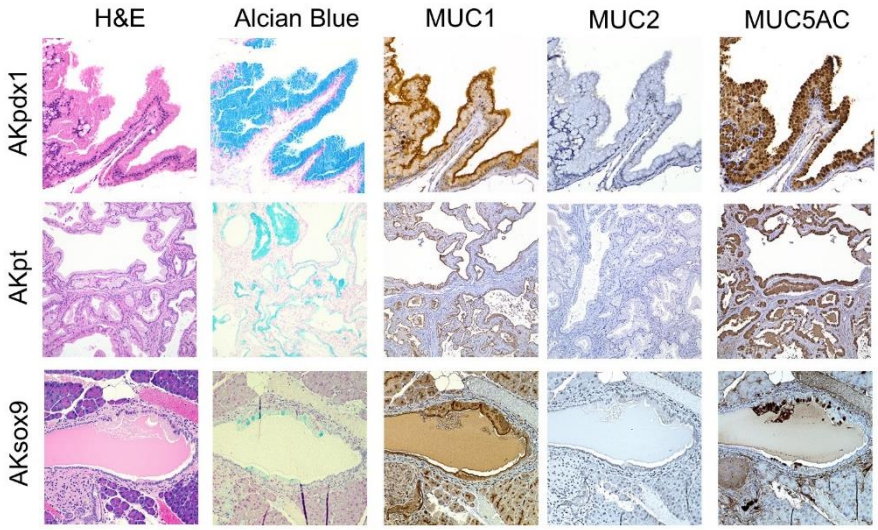

Figure 4. Morphological and immunohistochemical analysis of the preneoplastic lesions in AKpdx1, Akpt, and AKsox9 mice.

Representative images of H&E, Alcian blue, MUC1, MUC2 and MUC5AC staining of the pancreas from *Pdx1Cre;Kras*$^{LSL\text{-}G12D}$*;Acvr1b*$^{fl/fl}$ (AKpdx1), *Ptf1a*^{CreER}*;Kras*$^{LSL\text{-}G12D}$*;Acvr1b*$^{fl/fl}$ (AKpt), or *Sox9CreER;Kras*$^{LSL\text{-}G12D}$*;Acvr1b*$^{fl/fl}$ (AKsox9) mice. Magnification for images is 100x for AKpt and 200x for AKpdx1 and AKsox9 pancreata.

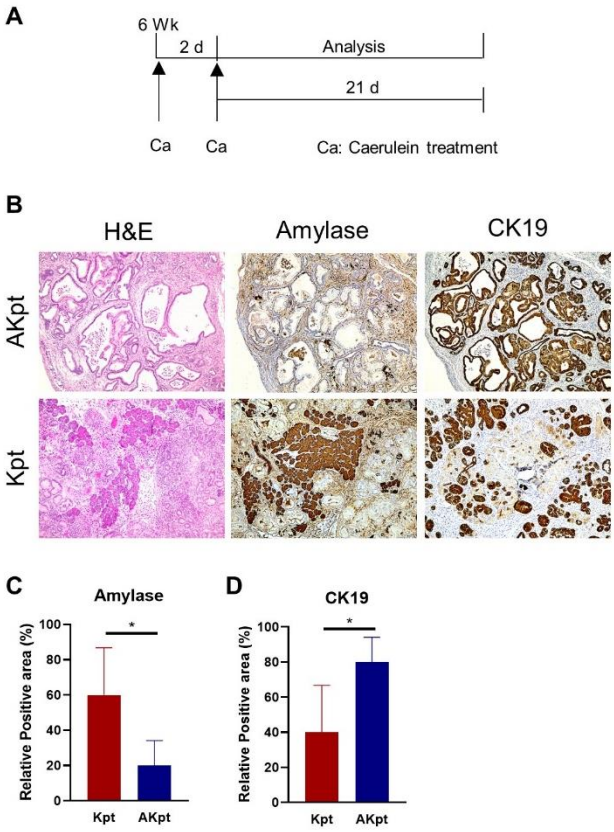

Figure 5. Caerulein treatment and *Acvr1b* loss promoted formation of IPMN-like lesions from Kras^{G12D}-expressing acinar cells.

(A) Schematic of the caerulein treatment plan - At 6 weeks of age, *Ptf1a^{CreER};Kras$^{LSL-G12D}$* (Kpt) (n=5) and *Ptf1a^{CreER};Kras$^{LSL-G12D}$;Acvr1b$^{fl/fl}$* (AKpt) (n=5) mice were treated with two rounds of caerulein (Ca) injections on alternative days and analyzed 21 days later. **(B)** Representative images of H&E staining of the pancreata from Kpt and AKpt mice treated with caerulein at day 21. Immunohistochemistry staining against Amylase or CK19 in AKpt or Kpt pancreata 21 days after caerulein treatment. Magnification for images is 20x. **(D-E)** Quantification of the Amylase-positive **(D)** or CK19-positive **(E)** pancreatic areas in the AKpt mice compared to the Kpt mice at 21 days after the caerulein treatment. $p<0.05$ by t-test.

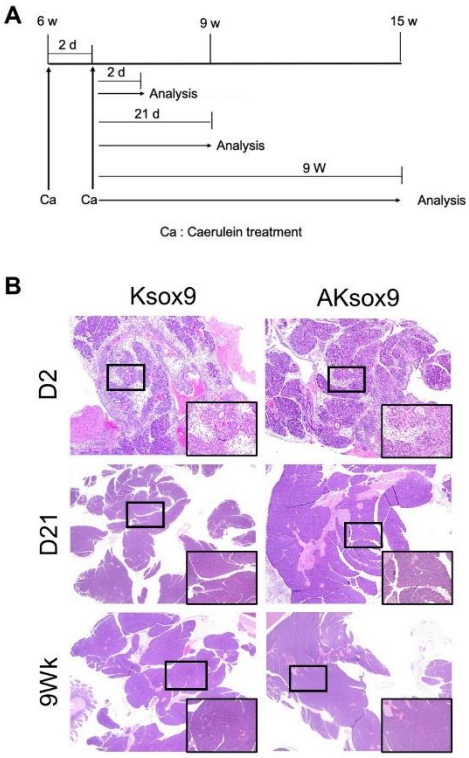

Figure 6. Kras expressing ductal cells have a low propensity to form PanINs after chemically-induced acute pancreatitis.

(A) Schematic of the caerulein treatment plan - At 6 weeks of age, *Sox9CreER;Kras*$^{LSL\text{-}G12D}$*;Acvr1b*$^{fl/fl}$ (AKsox9) (n= 4-6) and *Sox9CreER;Kras*$^{LSL\text{-}G12D}$ (Ksox9) (n= 3-4) mice were treated with two rounds of caerulein (Ca) injections on alternative days and analyzed at 2 or 21 days (d), or 9 weeks (w) later. **(B)** Representative images of H&E staining of the pancreas from Ksox9 or AKsox9 mice treated with caerulein at 2 or 21 days or 9 weeks post treatment. Magnification for main images is 20x and insets are 100x.

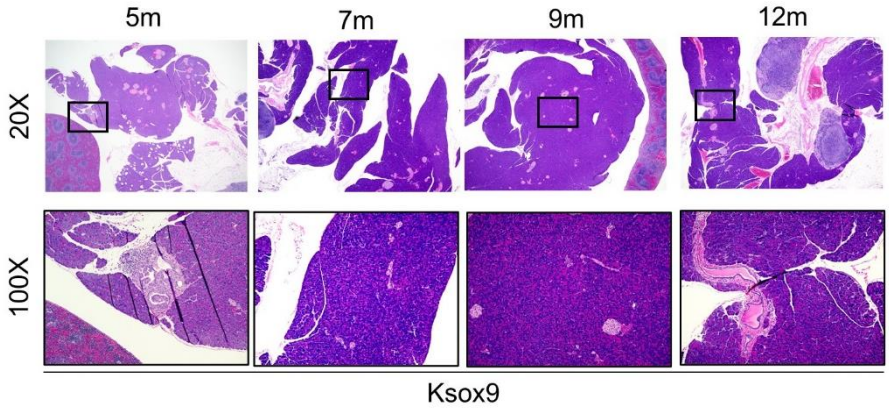

Figure S1. Ductal-cell-specific expression of oncogenic Kras results in few PanINs lesions.

H&E-stained sections of the pancreatic preneoplastic lesions of the *Sox9CreER;Kras*$^{LSL\text{-}G12D}$ (Ksox9) mice at 5, 7, 9, or 12 months of age. Magnification for main images is 20x and insets are 100x.

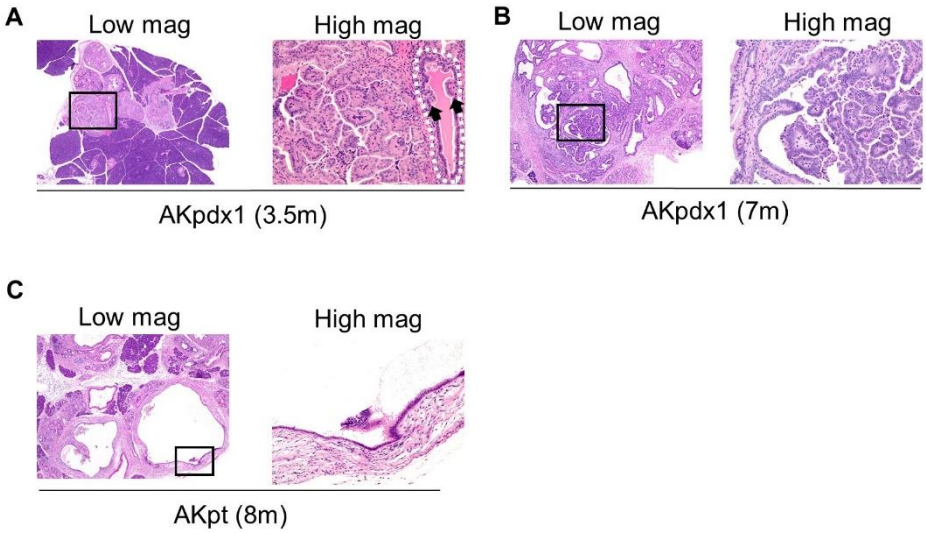

Figure S2. Histological images corresponding to MRI imaged pancreata. **(A-B)** Low and high magnification images of H&E-stained sections from the pancreas of *Pdx1Cre;Kras*$^{LSL\text{-}G12D}$*;Acvr1b*$^{fl/fl}$ (AKpdx1) mice at 3.5 **(A)** or 7 **(B)** months of age. High magnification depicts the papillary preneoplastic lesions within the dilated main pancreatic duct. Next to the dilated main pancreatic duct, there were PanIN lesions. The dashed white line denotes the main pancreatic duct dilation. Arrows indicate papillary neoplasms within the dilated main pancreatic duct. **(C)** Low and high magnification images of H&E-stained sections from *Ptf1a*^{CreER}*;Kras*$^{LSL\text{-}G12D}$*;Acvr1b*$^{fl/fl}$ (AKpt) pancreata at 8 months of age. Magnification for low-power images is 20x and for high power magnification is 100x.